

## Phase III of methane: Crystal structure and rotational tunneling

M. Prager<sup>a)</sup>

*Institut für Festkörperforschung, Forschungszentrum Jülich, D-52425 Jülich, Germany*

W. Press and B. Asmussen

*Institut für Experimentalphysik, Universität Kiel, D-24118 Kiel, Germany*

J. Combet

*Institut Laue-Langevin, F-38042 Grenoble Cedex 5, France*

(Received 14 November 2001; accepted 8 July 2002)

On the basis of the recently determined low temperature crystal structure of phase III of methane new high resolution tunneling spectra on 1.5% CH<sub>4</sub> dissolved in CD<sub>4</sub> are successfully described by two tunneling systems at sites with two-fold and mirror symmetry, respectively. The analysis is based on tunneling matrix elements. The octopole moments of the CH<sub>4</sub> impurities are found to agree with those of the CD<sub>4</sub> host molecules. *T* levels of molecules at *m* sites show different spin conversion times. Spectra of pure CD<sub>4</sub> III are reanalyzed and consistently explained assuming the presence of a small contamination of CD<sub>3</sub>H. © 2002 American Institute of Physics.

[DOI: 10.1063/1.1503336]

### I. INTRODUCTION

Methane is one of the simplest organic molecules and belongs to the most common materials on earth. Natural gas mainly contains methane. Furthermore large quantities of methane are present on the ocean floor in the form of clathrates. The binding to the host can be well studied via the dynamics of the guest molecules.<sup>1</sup> The simplicity of the molecule makes the pure material attractive as a prototype molecular crystal. The molecule can also act as a probe of some fundamental phenomena. Methane diluted in rare gases represents a model molecular defect. The interesting transition from isolated defects via defect clusters towards the pure crystalline material can be studied in great detail with increasing the methane concentration.<sup>2</sup> Similarly layer-by-layer absorption of methane on MgO is a well-studied example of a transition from a two-dimensional to a three-dimensional molecular solid.<sup>3</sup> The relationship of center-of-mass and orientational order is complex and not yet understood.<sup>4</sup>

Pure methane below the melting temperature  $T_m = 90.64$  K is the simplest organic crystal. It is of fundamental importance for the understanding of interactions in organic materials. An important step towards a comprehensive description of molecular crystals was done when intermolecular interactions were based on the transferable pair interaction potentials.<sup>5,6</sup> The alkanes with methane as the first member of the series were chosen as model compounds of single bonded pure hydrocarbons. Already this very simple material has a complex phase diagram with rather particular structures. On solidifying at atmospheric pressure methane CH<sub>4</sub> assumes the plastic cubic phase I, space group Fm3m,  $Z=4$ , down to  $T_c=20.4$  K. At this temperature the protonated material transforms into the partially ordered phase II, space group Fm3c,  $Z=32$ ,<sup>7</sup> which is stable down to the low-

est temperatures. The structure was predicted on the basis of octopole–octopole interaction of methane tetrahedra<sup>8</sup> and calculations were based on Lennard-Jones type pair interaction potentials proposed by Bartell.<sup>9</sup> The deuterated material undergoes the transition into phase II at a higher temperature  $T_{c1}=27.0$  K. A second transition to CD<sub>4</sub> III occurs at  $T_{c2}=22.1$  K.

The crystal structure of phase III remained a puzzle for a long time. To make progress the original theoretical description which was restricted to pure octopole–octopole interaction<sup>8</sup> was extended to include a crystal field and higher multipole interaction terms.<sup>10,11</sup> This so-called extended James–Keenan (EJK) model was used for more than two decades of intense theoretical work and explained many of the experimental observations in phase II of solid methane. On the basis of the EJK model various possible space groups of phase III were found by minimizing the crystal free energy under the assumption that phase III is a subgroup of phase II. The space group was predicted to be most likely  $P4_2/mbc$ .<sup>12</sup> However, a strong discontinuity of the order parameter at  $T_c$  indicated that the phase transition is definitively not of second order.

With the advent of very high-resolution neutron spectrometers a quantitative technique was available to determine rotational tunnel splittings of molecular ground states.<sup>13</sup> Since the tunnel splitting depends exponentially on the overlap of molecular wave functions it is the most sensitive probe of rotational potentials and intermolecular interactions. In solid methane the rotational potentials are weak enough to yield well resolved tunnel splittings. While the tunneling spectra of phase II<sup>14</sup> of pure methane are well understood, those of phase III<sup>15–17</sup> were in disagreement with the proposed space group  $P4_2/mbc$ .<sup>12</sup> The analysis of the spectra of CH<sub>4</sub> III and CD<sub>4</sub> III was, therefore, limited to a description by trial multisite models. There was the hope that conclusions about the number and the symmetries of sites de-

<sup>a)</sup>Electronic mail: m.prager@kfa-juelich.de

duced from tunneling experiments would have an impact on the solution of the structure problem.

Unbiased by theoretical predictions and solely based on recent diffraction data the crystal structure of phase III was then searched for with a state-of-the-art software package testing millions trial structures. Contrary to theoretical predictions the structure is not found among tetragonal space groups. It is very weakly orthorhombic with space group *Cmca*,  $Z=16$  molecules per unit cell and two inequivalent sites of twofold and *m* symmetry, respectively, and equal occurrence probabilities.<sup>18</sup> Despite the fact that the correct description as concerns the site symmetries and multiplicities was among the models extracted from tunneling spectra,<sup>16</sup> the information was not sufficiently unique, due to unresolved and overlapping lines, to contribute decisively to solving the structure. Now the newly found crystal structure confirms the respective model describing the tunneling spectra of methane under pressure.<sup>16</sup>

The main section of the paper is devoted to a new high-resolution measurement of tunneling splittings of CH<sub>4</sub> molecules matrix isolated in a CH<sub>4</sub> host lattice. Similarities with methane under pressure will be discussed. Furthermore we reanalyze tunneling spectra from phase III of deuterated methane.<sup>15</sup>

## II. THEORY

The theory of single particle rotation of spherical tops is based on the Hamiltonian  $H$  of the three-dimensional rotor with rotational constant  $B$  in a potential  $V(\omega_E)$

$$H = -B\nabla^2 + V(\omega_E), \quad (1)$$

with  $\omega_E$  representing the Eulerian angles. The potential may be obtained from *ab initio* calculations based on the crystal structure and fundamental intermolecular interactions. For use in Eq. (1) it is expanded into rotator functions.<sup>13</sup> The stronger the rotational potential the more the calculated tunnel splitting depends on the precision the wave function is described. For example, the calculated tunnel splitting of ordered methane molecules in phase II with their rather weak barrier of about 35 meV changes by about 40% when a simple Gaussian wave function is weakly modified by multiplication with a symmetry allowed polynomial.<sup>19</sup> For lower site symmetries these problems may become even more important. The lower the symmetry of the three-dimensional potential the larger the number of symmetry allowed terms of its Fourier expansion. The terms are too many to determine their amplitudes from the few observed transitions. If the fit algorithm can be used on a known crystal structure and interatomic interaction potentials the number of free fit parameters is reduced to the number of pair potential parameters.<sup>20</sup>

The symmetry and the shape of the rotational potential are contained in the overlap matrix elements of the rotational wave functions in the potential  $V(\omega_E)$ . Thus they may be used almost equally well as appropriate parameter of the problem. This approach has no link with the crystal frame and does not allow to get the orientation of the rotational potential. In the case of no symmetry the four possible 120°

TABLE I. Symmetry properties of tunneling matrix elements  $h_i$  and  $H_i$  for 120° and 180° overlap for the site symmetries present in the space group *Cmca* of phase III of methane.

Site symmetry	Matrix elements						$T_i \rightarrow T_j$ intensities
2	$h_1 = h_2$	$h_3 = h_4$	$H_x$	$H_y$	$H_z$	const	
m	$h_1$	$h_2$	$h_3 = h_4$	$H_x = H_y$	$H_z$	depend on $h_i$	

overlap matrix elements  $h_i$  related with rotations of the tetrahedron about its four threefold axes are all different, similarly the three possible 180° overlap matrix elements  $H_i$  related with rotations of a tetrahedron about its twofold axes. In such conditions the tunnel split librational ground state is a quintet ( $A, T_1, T_2, T_3, E$ ) with nine allowed transitions of usually different energy transfers. With increasing site symmetry T-levels become degenerate and the number of transitions is finally reduced to two for a tetrahedral site symmetry. In the actual case we need the results for twofold and mirror symmetry. While intensities of  $T_i \rightarrow T_j$  transitions may depend on matrix elements the  $A \rightarrow T_i$  and  $T_i \rightarrow E$  intensities are constant with a ratio 1.2. All these properties are shown in Table I. They<sup>13</sup> are included into the computer program to use to analyze the measured spectra. This program also allows for the first time to test the effect of individual  $H_i$ .

The analysis of CD<sub>4</sub> spectra will deal with substitutional CD<sub>3</sub>H defects in a CD<sub>4</sub> matrix. The tunneling spectra and transition matrix elements of the symmetric top CD<sub>3</sub>H do not have a firm theoretical basis.<sup>21</sup> In analogy with the light symmetric top NH<sub>3</sub>D<sup>22–24</sup> CD<sub>3</sub>H is considered as a one-dimensional rotor and assigned a single tunneling transition line per site.

## III. EXPERIMENT

### A. Sample preparation

The isotopic purity of the CD<sub>4</sub> host material was 98%, that of the CH<sub>4</sub> guest molecules 99.99%. The chemical purity of both gases was higher than 99.99%. 1.5% CH<sub>4</sub> in CD<sub>4</sub> was prepared in a gas mixing chamber equipped with pressure sensors. A total of 12 liters at standard conditions was condensed through a heated capillary into a flat aluminum cell of dimensions 30×40×15 mm<sup>3</sup>. The sample preparation took about 40 minutes. This time was needed due to the weak thermal coupling between sample and cryostat and the correspondingly slow removal of the heat of condensation. The sample was oriented at 45° with respect to the neutron beam direction.

The total scattering probability of the sample was 32%. The larger part of this, about 20%, is scattering by the deuterated matrix and represents background. Only 12% represents scattering from the CH<sub>4</sub> guest molecules. Multiple scattering mainly perturbs the  $Q$ -dependence of elastic and inelastic intensities but not the relative intensities of tunneling lines we are interested in.

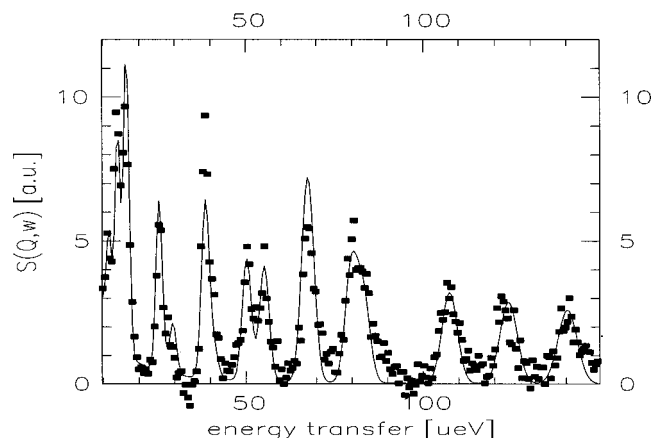


FIG. 1. Spectrum of 1.5%  $\text{CH}_4$  in  $\text{CD}_4$  with background subtracted. Data taken at the backscattering instrument IN10B, ILL, Grenoble. Energy resolution about  $1 \mu\text{eV}$ . Sample temperature  $T=4.2 \text{ K}$ . ■■■: experiment; —: fit based on the  $Cmca$  structure of phase III (Ref. 18).

## B. Tunneling spectroscopy

To cover a wide range of energy transfers backscattering with a variable temperature monochromator was used. The only appropriate instrument is IN10B of the ILL, Grenoble, France. Even there it is impossible to cover the wanted range of energy transfers with one monochromator crystal. Thus IN10B was used with two different monochromator crystals,  $\text{KCl}[200]$  and  $\text{NaCl}[111]$ . The two setups allowed us to explore the energy regime  $-7 \mu\text{eV} \leq E \leq 180 \mu\text{eV}$ . The energy resolution was about  $1.5 \mu\text{eV}$ . The data acquisition was done in three steps. The first scan was restricted to the regime below  $90 \mu\text{eV}$  to be sure not to damage the  $\text{KCl}$  monochromator by too high a temperature. The second scan reached an upper energy transfer of  $123 \mu\text{eV}$  using the same monochromator at the highest possible temperature ( $T=800 \text{ K}$ ) where the Debye–Waller factor had already reduced the incoming neutron flux by about a factor of 2. Changes of neutron flux at the sample were eliminated by normalization. A further extension of the energy range required the use of the  $\text{NaCl}$  monochromator. The lowest possible temperature of about  $100 \text{ K}$  corresponds to an energy transfer of  $120 \mu\text{eV}$ . High energy transfers above  $180 \mu\text{eV}$  were prohibited by the shielding of the neutron guide which limits the maximum accessible Bragg angle of the deflector crystal. Since the lattice parameters of both monochromator crystals are larger than that of the silicon only downscattering processes can be observed. Full squares in Fig. 1 show data accumulated during  $36 \text{ h}$ .

The background of pure  $\text{CD}_4$  was measured only in the vicinity of the elastic liner. At energies above the tunneling transitions of  $\text{CD}_4$  there is a high but constant background which amounts to about 30% of the most intense inelastic line of the  $\text{CH}_4$  guest molecules. Fortunately, all tunneling transitions of  $\text{CH}_4$  occur at energies higher than those of the  $\text{CD}_4$  host matrix.

To get overlap of the partial spectra the  $\text{NaCl}[111]$  monochromator had to be used at temperatures which were lower than recommended. At the corresponding lowest energy transfer droplets of liquid nitrogen in the cooling

gas inhibited a stabilization of the monochromator temperature. Fortunately only  $A \rightarrow T$  transitions of methane molecules at two-fold sites fall into this partial spectrum. The only independent information contained in these lines concerns the magnitude of the corresponding  $180^\circ$  overlap matrix element  $\bar{H}$ .

## IV. RESULTS AND DISCUSSION

The experiment was proposed at a time when the crystal structure of phase III of methane was not yet known and was intended to contribute to its solution. Already in its early days neutron tunneling spectroscopy of three-dimensional rotors was used in a similar way as Raman spectroscopy to determine site symmetries. The first material where the fine structure of the librational ground state was analyzed was ammoniumperchlorate. An accidental degeneracy of  $T$ -levels led to an apparent discrepancy which later could be ruled out when the fit was based on overlap matrix elements  $h_i$ .<sup>25</sup> The same advanced method had to be used in other complex cases such as methane absorbed as a monolayer on the  $\text{MgO}[100]$  surface<sup>26</sup> to extract a site symmetry. Because of the obvious advantages the present data analysis is also based on tunneling matrix elements.

### A. 1.5% $\text{CH}_4$ in $\text{CD}_4$

With the best energy resolution of  $\delta E = 5 \mu\text{eV}$  available in 1988 for the contiguous energy range up to  $200 \mu\text{eV}$  a sample with 4%  $\text{CH}_4$  in  $\text{CD}_4$  was studied. This was done on the cold time-of-flight spectrometer IN5 of the ILL, Grenoble, using an incoming wavelength of  $\lambda = 13 \text{ \AA}$ . Data had to be accumulated for three days due to the low flux.<sup>17</sup> However, even at the highest energy transfers where time-of-flight spectrometers show the best energy resolution the tunneling lines were still not fully resolved. A model with three sites of different weights yield the best fit. A simpler two-site model used for methane under pressure<sup>16</sup> showed less good results. The improved energy resolution of the present experiment reveals many more details, especially at low energy transfers. The increased inelastic structure factor at the larger momentum transfer of a backscattering instrument could not compensate for its low flux and high background, however. The statistics of the spectrum of Fig. 1 is still relatively poor. The inelastic intensity is limited by the low concentration of  $\text{CH}_4$  guest molecules and spreads out over the large energy range up to  $150 \mu\text{eV}$ . Despite the low concentration of 1.5% guest molecules disorder still gives rise to a significant width of the tunneling bands. Inhomogeneous line broadening  $\Gamma$  usually is proportional to the energy transfer<sup>27</sup>

$$\Gamma(\hbar\omega) = \Gamma_0(1 + \alpha\hbar\omega), \quad (2)$$

and affects the quality of data especially at large energy transfers. In our case  $\alpha = 0.018 \mu\text{eV}^{-1}$ . Thus, at large energy transfer the energy resolution is too good for a sample of the given quality. Inhomogeneous line broadening is found even in pure methane  $\text{CH}_4$ .<sup>28</sup> Pure methane may be described as an “alloy” with molecules in the  $A$ ,  $T$ , and  $E$  tunnel states. Populations of rotational levels, in particular also of neighbors of a given molecule change with temperature. The reduction of the octopole moment of molecules in the ground

TABLE II. Tunneling matrix elements  $h_i$  and average value of  $\bar{H}$  for 120° and 180° overlap, respectively, as derived by fits to data of the cited samples assuming two equally populated sites of twofold and  $m$ -symmetry as required by the  $Cmca$  space group of phase III. Potential strengths  $V_3$  are derived in a one-dimensional model for the individual tunnel matrix elements. There may be systematic deviations from the real barrier due to the wrong dimensionality of the model. See the text.

	2-site			$m$ -site				Sample/Ref.
	$h_1=h_3$	$h_2=h_4$	$\bar{H}$	$h_1$	$h_2$	$h_3=h_4$	$\bar{H}$	
$h_i[\mu\text{eV}]$	-19.99	-11.82	0.80	-2.09	-16.55	-6.33	0.056	CH <sub>4</sub> in CD <sub>4</sub>
$V_3[\text{meV}]$	16.9	20.6		34.4	18.2	25.2		= this exp.
$h_i[\mu\text{eV}]$	-24.3	-15.2	3.9	-3.5	-20.5	-9.4	1.0	CH <sub>4</sub> (0.6 kbar) (Ref. 16)
$V_3[\text{meV}]$	15.7	18.8		29.8	16.8	22.2		
$h_i[\mu\text{eV}]$	-20.0	-12.0	.1	-2.7	-16.5	-7.4	3.6	CH <sub>4</sub> (1.0 kbar) (Ref. 16)
$V_3[\text{meV}]$	16.9	20.5		32.0	18.2	24.0		
$h_i[\mu\text{eV}]$	-15.5	-8.6	1.0	-2.0	-12.9	-5.5	0.0	CH <sub>4</sub> (1.8 kbar) (Ref. 16)
$V_3[\text{meV}]$	18.7	22.9		34.5	20.0	26.3		
$h_i[\mu\text{eV}]$	-1.116	-0.524	...	-0.167	-0.733	-0.532	...	CD <sub>4</sub> (Ref. 15)
$V_3[\text{meV}]$	16.8	20.1		25.6	18.6	20.0	...	
$h[\mu\text{eV}]$	-17.7							CH <sub>4</sub> (Ref. 14)
$V_3[\text{meV}]$	17.8							

state softens the rotational potential at low temperatures. Thus the tunnel splitting measured at  $T \approx 5$  K increases when cooling to  $T = 0.2$  K by about 12%. A qualitatively similar disorder is obtained in CD<sub>4</sub> when replacing some CD<sub>4</sub> by CH<sub>4</sub>. With a finite probability the studied CH<sub>4</sub> molecules have other CH<sub>4</sub> neighbors which modify the local symmetry and interaction strength.

Transition matrix elements describe the relative intensities of tunneling lines in case of equal population of the tunneling sublevels. For large tunnel splittings population factors may change these intensities. Since equilibration with the phonon bath requires spin flips, slow spin conversion times  $\tau$  may lead to time dependent populations. Large differences of  $\tau$  may even cause population inversion.<sup>28,29</sup> Spin conversion times of methane strongly depend on the concentration of oxygen impurities, the sample temperature, the thermal history, etc.<sup>28,30</sup> Blockage of spin diffusion is believed to be the most important process preventing equilibration.<sup>28</sup> Since the accessible energy range in the present backscattering experiment does not allow to determine the unknown population factors experimentally by comparison of the Stokes and Antistokes transitions we describe the intensities by transition matrix elements and attribute deviations as due to differences of spin conversion times on the slow way to new thermal equilibrium.

The assignment of transitions is guided by the crystal structure of phase III.<sup>18</sup> The equidistant three lines at high energy transfers ( $\hbar\omega \approx 100 \mu\text{eV}$ ) are identified as the  $T_i \rightarrow A$  transitions of the sites with twofold symmetry. This assignment determines all other tunneling transitions of this site. Due to the weak potential barrier the 180° overlap matrix elements  $H_i$  cannot be neglected. Finite  $H_i$  cause a shift of all the three high energy transitions. Signs and sizes of the tunnel matrix elements are used according to the convention of Ref. 13. Unfortunately the scatter of the data did not allow us to extract  $H_i$ 's individually but only an average  $\bar{H}$ . Due to the fact that all  $T_i \rightarrow A$  transitions are found in the regime accessible with the second monochromator crystal even the

determination of  $\bar{H}$  is connected with a large systematic error.

The remaining inelastic intensity is attributed to transitions of methane molecules at  $m$ -sites. Starting with assigning the strongest unexplained inelastic peak to a  $T_i \rightarrow A$  transition a number of combinations of lines was explored. Again the 180° overlap matrix elements  $H_i$  cannot be neglected. Due to instabilities of the fit with independent  $H_i$  the final fit had again to be performed under the restriction of all  $H_i$  being equal.

Fit parameters are presented in Table II. The small matrix element  $h_1$  at the  $m$  site shows that there is one hard axis of rotation. Since  $h_1$  is unique this axis must lie in the mirror plane. To decide which one of the two it is requires *ab initio* calculations which link the molecular and the crystal frame.

The fit is shown as solid line in Fig. 1. Some intensities deviate from the assumption of equal populations of all levels. Thermal equilibrium at  $T = 2.0$  K would allow for differences in thermal population up to  $\exp[-11.6(\text{K/meV})(0.21 \text{ meV}/2 \text{ K})] \sim 0.3$  where the 0.21 meV represent the largest  $A - E$  splitting of the two-tunnel systems. Only lines resulting from downscattering from the same level must show intensity ratios characteristic of transition matrix elements. Unfortunately, such  $E \rightarrow T_i$  transitions strongly overlap. We find that all excited levels of the methane molecules at the twofold site are equally populated. The two regimes in which the intensities are fitted rather badly are related to transitions from  $T_i$  levels of methane molecules at  $m$  sites ( $T_1 \rightarrow A, T_2 \rightarrow A$ ). An increased population of  $T_1$  and a depopulation of  $T_2$  significantly improve the fit. Thus we conclude that  $T_1$  states convert more slowly,  $T_2$  states faster compared to the average behavior.

## B. CD<sub>4</sub>III

The original interpretation of the tunneling data of pure CD<sub>4</sub> III involved more complex multisite models.<sup>15</sup> The description by the two-site model developed for methane under



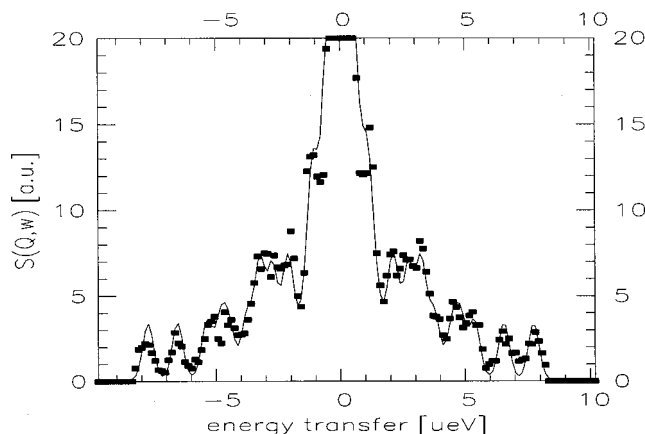


FIG. 2. Neutron spectrum of  $\text{CD}_4$  measured at high-resolution at the back-scattering instrument IN10B, ILL, Grenoble. Energy resolution  $0.4 \mu\text{eV}$ . Sample temperature  $T=4.2 \text{ K}$ . ■-■-■: experiment; —: fit.

pressure was unsatisfactory.<sup>15</sup> After confirmation of this model by the crystal structure determination<sup>18</sup> we have to find a reason for the apparent inconsistency.

When studying the isotope effect of almost free methane rotors isolated in rare-gas matrices the presence of a significant amount of  $\text{CD}_3\text{H}$  and—less importantly— $\text{CD}_2\text{H}_2$  in  $\text{CD}_4$  was observed.<sup>29</sup> Thus the actual discrepancy is tentatively attributed to the presence of transition of  $\text{CD}_3\text{H}$ . The tunneling spectrum of pure  $\text{CD}_3\text{H}$  measured at an energy resolution of  $\sim 1 \mu\text{eV}$  showed a broad inelastic intensity below  $14 \mu\text{eV}$ .<sup>21</sup>

Weakly deuterated ammonium salts contain the light symmetric top  $\text{NH}_3\text{D}$  due to H–D exchange in a binomial probability distribution. Their tunnel spectra differ from those of the fully protonated material by a single additional line and may be ascribed to one-dimensional rotation of the  $\text{NH}_3\text{D}$  rotor around its symmetry axis.<sup>22–24</sup> The relative tunnel splittings of  $\text{NH}_4$  and  $\text{NH}_3\text{D}$  can be reasonably well obtained from the same  $120^\circ$  overlap matrix element  $h$ . If  $\hbar\omega_{(T \rightarrow E)} = 4h$  for three-dimensional rotation in a tetrahedral field then  $\hbar\omega_t = 3h$  for one-dimensional rotation in the same potential. In phase III of methane  $120^\circ$  overlap matrix elements become different. While most intensity of  $\text{CD}_3\text{H}$  rotors coincides with low energy tunneling bands of  $\text{CD}_4$  a new line from molecules at the two-fold site is expected around  $\sim 2.7 \mu\text{eV}$ . This is exactly the energy regime where the quality of the fit is less good if only  $\text{CD}_4$  is taken into account. We can estimate the presence of  $\sim 8\%$   $\text{CD}_3\text{H}$  molecules from the quoted 98% isotopic purity of the supplied  $\text{CD}_4$  gas. Since the scattered intensity is concentrated into a single line there should be rather similar intensity to that of tunneling transitions of  $\text{CD}_4$  molecules where the much larger total intensity (92%  $\text{CD}_4$ ) is distributed over 16 tunneling transitions (not all of them resolved). A fit of the spectrum of the fully deuterated material including *one* additional tunneling line at  $\hbar\omega_t = 2.65 \mu\text{eV}$  describes the data well (Fig. 2). The overlap tunneling matrix elements of  $\text{CD}_4$  are shown in Table II.

For further semiquantitative estimate we adopt a one-dimensional approach where each individual tunnel matrix

element  $h_i$  is taken as characteristic of the corresponding one-dimensional cut through the three-dimensional potential surface. For one-dimensional rotation the tunnel splitting is  $\hbar\omega_{ti} = 3h_i$ . In the simplest model it is determined by a pure  $\cos 3\varphi$  potential. This way the potential strengths  $V_{3i}$  shown in Table II are obtained from the Mathieu equation. The procedure allows us to compare the different methane samples very roughly on the level of rotational potentials without assumption on scaling rotational constants. One finds that the rotational potential at the twofold site of “ $\text{CH}_4$  in  $\text{CD}_4$ ” and “pure  $\text{CD}_4$ ” are very similar in strength and shape (Table II). Similar potentials imply similar octopole moments of the two isotopic methanes in phase III.

In case of molecules at  $m$ -sites the matrix elements related with the stronger barriers or the harder axes of rotation are somewhat smaller than for  $\text{CH}_4$  impurities in  $\text{CD}_4$ . The shapes of the respective three-dimensional potential surfaces are slightly different. Either such changes occur at the  $m$ -site only or the exponential increase of the sensitivity of the tunnel probe with increasing barrier height makes them only observable for the higher barriers. It may also be that the one-dimensional model breaks down.

### C. $\text{CH}_4$ under pressure

$\text{CH}_4$  under pressure represents the “cleanest situation.” There are no effects from interacting impurities which perturb the results of both  $\text{CH}_4$  matrix isolated in  $\text{CD}_4$  (dimers etc.) and pure  $\text{CD}_4$  which always contains  $\text{CHD}_3$ . The tunnel matrix elements obtained for the two-site model are consistent with the crystal structure and are reproduced<sup>15</sup> in Table II for the three investigated pressures. A comparison of overlap matrix elements shows that  $\text{CH}_4$  matrix isolated in  $\text{CD}_4$  III correspond to pure  $\text{CH}_4$  III at a pressure  $p = 1.0 \text{ kbar}$  for both crystallographic sites.

## V. CONCLUSION AND OUTLOOK

Tunneling spectra measured in phase III of solid methane can be explained on the basis of the recently determined crystal structure with the space group  $Cmca$ .<sup>18</sup> Vice versa they confirm this crystal structure. The knowledge of the crystal structure allows us to relate deviations of the observed intensities of  $\text{CH}_4$  matrix isolated in  $\text{CD}_4$  III from those calculated from matrix elements with different spin conversion times of different tunneling sublevels. In case of pure  $\text{CD}_4$  III the presence of  $\text{CD}_3\text{H}$  impurities accounts for unexplained tunneling intensity.

The presented description of tunneling spectra by overlap matrix elements is phenomenological and a first step. It is a task for theory to relate the overlap matrix elements via wave functions with the low symmetry three-dimensional rotational potential  $V(\omega_E)$  and to express  $V(\omega_E)$  on the basis of the crystal structure by intermolecular atom–atom potentials. The calculated rotational potential will yield new information as the orientation of soft and hard axes of rotation in the crystal frame. If overlap matrix elements can be based on the fundamental properties of pair potential parameters even quantities with small values like the  $180^\circ$  matrix elements (which the experiment delivers with huge error bars only)

can be determined rather well. Eventually, an improvement of the pair potential parameters used so far successfully for methane<sup>9</sup> might result from such a calculation.

It is assumed so far (and rather likely) that all partially deuterated methanes at low temperature crystallize within the space group *Cmca* of CH<sub>4</sub> III. However, the molecular symmetries of the monosubstituted spherical tops CH<sub>3</sub>D and CD<sub>3</sub>H do not match with a two-fold site symmetry. This must lead to interesting quantum disorder, an effect worth studying.

Above a pressure of  $p \sim 4.5$  kbar methane CH<sub>4</sub> transforms into phase IV. So far this phase has not been studied by high resolution spectroscopy. The progress in understanding the crystal structure and dynamics of phase III of methane is a motivation to proceed to phase IV and other phases of the simplest organic solid. It is a technical challenge but looks feasible to get the required high and homogeneous pressure for sufficiently large sample volumes.

## ACKNOWLEDGMENT

The authors thank A. Hüller for very helpful discussions.

- <sup>1</sup>C. Gutt, W. Press, A. Hüller, J. Tse, and H. Casalta, J. Chem. Phys. **114**, 4160 (2001).
- <sup>2</sup>B. Asmussen, D. Balszunat, M. Prager, W. Press, C. J. Carlile, and H. Büttner, J. Chem. Phys. **103**, 6880 (1995).
- <sup>3</sup>J. Larese, Physica B **248**, 297 (1998).
- <sup>4</sup>Y. Ozaki, M. Prager, and B. Asmussen, J. Phys. Chem. Solids **60**, 1523 (1999).
- <sup>5</sup>D. E. Williams, J. Chem. Phys. **47**, 4680 (1967).
- <sup>6</sup>A. I. Kitaigorodskii and K. V. Mirskaya, Sov. Phys. Crystallogr. **9**, 137 (1964).
- <sup>7</sup>W. Press, J. Chem. Phys. **56**, 2597 (1972).
- <sup>8</sup>J. M. James and T. A. Keenan, J. Chem. Phys. **31**, 12 (1959).
- <sup>9</sup>L. S. Bartell, J. Chem. Phys. **32**, 827 (1960).
- <sup>10</sup>H. Yasuda, Prog. Theor. Phys. **45**, 1361 (1971).
- <sup>11</sup>T. Yamamoto, Y. Kataoka, and K. Okada, J. Chem. Phys. **66**, 2701 (1976).
- <sup>12</sup>K. Maki, Y. Kataoka, and T. Yamamoto, J. Chem. Phys. **70**, 655 (1979).
- <sup>13</sup>W. Press, *Single Particle Rotations in Molecular Crystals, Springer Tracts in Modern Physics* (Springer, Berlin, 1981), Vol. 81.
- <sup>14</sup>W. Press and A. Kollmar, Solid State Commun. **17**, 405 (1975).
- <sup>15</sup>M. Prager, W. Press, and A. Heidemann, J. Chem. Phys. **75**, 1442 (1981).
- <sup>16</sup>M. Prager, W. Press, and C. Vettier, J. Chem. Phys. **77**, 2577 (1982).
- <sup>17</sup>M. Prager and W. Press, J. Chem. Phys. **92**, 5517 (1990).
- <sup>18</sup>M. Neumann, W. Press, B. Asmussen, M. Prager, and R. Ibberson, Phys. Rev. Lett. (2002) (to be published).
- <sup>19</sup>A. Hüller and J. Raich, J. Chem. Phys. **71**, 3851 (1979).
- <sup>20</sup>D. Smith, J. Chem. Phys. **86**, 4055 (1987).
- <sup>21</sup>K. Lushington, K. Maki, J. A. Morrison, A. Heidemann, and W. Press, J. Chem. Phys. **75**, 4010 (1981).
- <sup>22</sup>H. Büttner, G. Kearley, and B. Frick, Chem. Phys. **214**, 425 (1997).
- <sup>23</sup>M. Prager, P. Schiebel, M. Johnson, H. Grimm, H. Hagdorn, J. Ihringer, W. Prandl, and Z. Lalowicz, J. Phys.: Condens. Matter **11**, 5483 (1999).
- <sup>24</sup>M. Prager, P. Schiebel, and H. Grimm, J. Chem. Phys. (to be published).
- <sup>25</sup>M. Prager and W. Press, J. Chem. Phys. **75**, 494 (1981).
- <sup>26</sup>J. Larese, J. Hastings, L. Passell, D. Smith, and D. Richter, J. Chem. Phys. **95**, 6997 (1991).
- <sup>27</sup>S. Grondy, M. Prager, W. Press, and A. Heidemann, J. Chem. Phys. **85**, 2204 (1986).
- <sup>28</sup>A. Heidemann, K. Lushington, J. A. Morrison, K. Neumaier, and W. Press, J. Chem. Phys. **81**, 5799 (1984).
- <sup>29</sup>B. Asmussen, D. Balszunat, W. Press, M. Prager, C. J. Carlile, and H. Büttner, Physica B **202**, 224 (1994).
- <sup>30</sup>S. Grieger, H. Friedrich, K. Guckelsberger, R. Scherm, and W. Press, J. Chem. Phys. **109**, 3161 (1998).